URSI GASS 2021, Rome, Italy, 28 August - 4 September 2021

A Multi-port Formulation for Electromagnetic Coupled *Auto-tuning* RFID Antennas

Nicoletta Panunzio*(1) and Gaetano Marrocco(1)
(1) University of Roma Tor Vergata, DICII, Via del Politecnico,1, 00133, Roma, Italy

Abstract

Arrangements of closely coupled UHF RFID tags are common in the industrial labelling and sensing of vaccines, and of stacks of small objects in general. The mismatch effect of coupling can be mitigated by the new family of *auto-tuning* ICs having a dynamic internal impedance. A network model is here introduced for the first time with the purpose to predict the response of sets of coupled *auto-tuning* tags. The analytical model reduces to a closed form description of the tags retuning capability in the particular case of two items in symmetric arrangement. Preliminary experimentations corroborate the theoretical dynamic responses of the ICs w.r.t. variable inter-tag distance. The model can be useful for a better understanding of the potentiality of this class of devices and to optimize their performance for advanced identification and sensing.

1 Introduction

Dense distributions of electronic labelled objects by means of Radiofrequency Identification (RFID) tags working in the UHF band (860-960 MHz) occur in several industrial scenarios, like the cold chain of vaccines (Fig. 1.a) [1],[2], apparel [3] and stacks of documents [4]. The resulting electromagnetic coupling may cause impedance mismatch and, more in general, a degradation of performance [5]. The recently introduced new family of *auto-tuning* RFID ICs [6],[7],[8] partially mitigate this problem by resorting to an automatic retuning of the internal impedance to partially compensate the variation of the local boundary conditions. This happens when the tag interacts with different materials [9] or when it is placed on different body regions and different users [10] (in the case of *Epidermal* RFID tags [11]). In this way, the power the antenna delivers to the IC is kept stable, thus making the communication performance rather insensitive with respect to slight modifications of the nearby environment. Moreover, the retuning process also returns an integer indicator that provides information on the retuning effort. This number can be also used as an indirect metrics to sense the dielectric change of the tagged object or of the local environment, such as in the recognition of liquid compounds [12] or of the nearby materials [13].

A general theoretical electromagnetic model of the *auto-tuning* RFID ICs has been presented in [12] for the case of a single-chip tag, and further developments can be found in [9] for near-field reader-to-tag communication. However, estimating the response of multiple *auto-tuning* tags placed at a near-field distance, where the inter-antenna coupling can not be neglected, is still an open challenge.

Electromagnetic coupled RFID tags can be regarded as a multiport scatterer. They were first investigated in [14] and [15], and applied to multi-sensing purposes in [16] and [17]. However, the available models are limited to RFID ICs with static impedance, and hence they do not apply to *auto-tuning* chips, whose input impedance is instead the result of the inter-tag coupling itself.

This paper addresses for the first time the formulation of the *auto-tuning* effects when the behavior of each chip is dependent on closely interacting ones. Formulas for the case of two coupled antennas are deduced by the theory of multi-port scatterers and some preliminary results permits to get more inside the phenomenon.

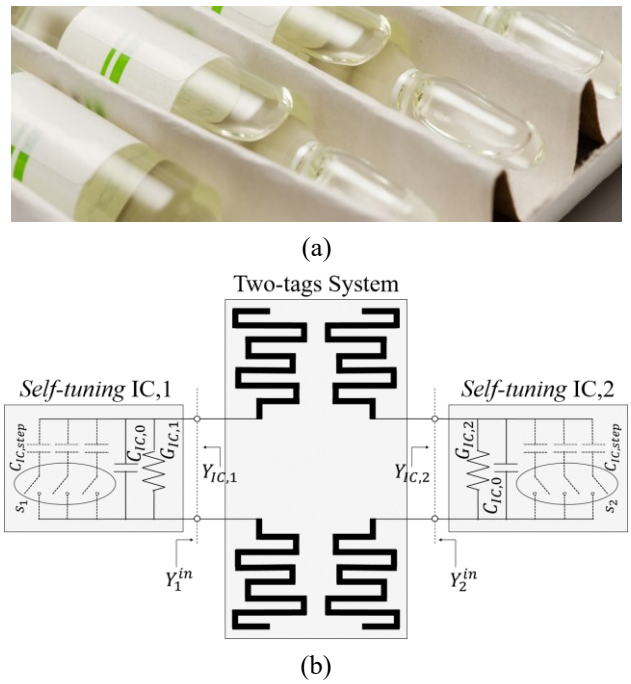

Figure 1. (a) An example of close coupled multitude of RFID tags over vaccines [18]. (b) Schematic representation of a two-tags antenna system, with esplicit depiction of the internal matching network of the connected *auto-tuning* ICs.

2 *Auto-tuning* Model for Coupled RFID Tags

With reference to Fig. 1.b, let $Y_{IC,n} = G_{IC,n} + jB_{IC,n}(s)$ denote the dynamic admittance of the IC at the n-th port, and $Y_n^{in}(\psi) = G_n^{in}(\psi) + jB_n^{in}(\psi)$ the input admittance of the n-th tag antenna. The latter depends on an external parameter $\psi(t)$, which is intended as a variable boundary condition that affects the antenna performance due to an

alteration of the antenna-IC impedance matching. To mitigate this effect, an *auto-tuning* IC includes a varactor device in the analog front-end that can be modelled as a parallel of a fixed resistance and a variable capacitor, which in turn can be seen as a switchable ladder of N identical capacitors. Starting from a minimum value $C_{IC,0}$, the overall capacitance is modulated with incremental steps $C_{IC,step}$ according to the law $C_{IC}(s_n) = C_{IC,0} + s_n\, C_{IC,step}$, where s_n is the number of the connected equivalent capacitors in each IC equivalent tuning scheme. Thanks to this internal logic, the chip dynamically reconfigures its own susceptance in order to compensate the varying antenna's susceptance, so that:

$$\left|B_{IC,n}(s_n) + B_n^{in}(\psi)\right| = 0\,. \tag{1}$$

By inverting (1), the retuning indicator s_n is found to be directly proportional to $B_n^{in}(\psi)$:

$$s_n(\psi) = S_{min} + \\ +nint\left[-\frac{1}{C_{IC,step}}\left(C_{IC}(S_{min}) + \frac{B_n^{in}(\psi)}{\omega}\right)\right]. \tag{2}$$

This parameter, also denoted as *sensor code, is* returned by the tag following a standard RFID query. Eq. (2) includes the constraint $S_{min} \le s_n \le S_{max}$ that is specific of the particular IC implementation. Namely, a saturation of the sensor code value occurs outside this range, and the retuning effort of the chip becomes ineffective. The sensor code, in general, varies depending on the geometrical arrangement of the tags and on the proximity to other objects [19], [20], and provides information on the matching extent of the set of ICs of the multichip system. Furthermore, when coupled tags are involved, the input susceptance of the n-th antenna not only depends on the whole multi-tag arrangement and the local environment, but also on the other ICs' susceptance.

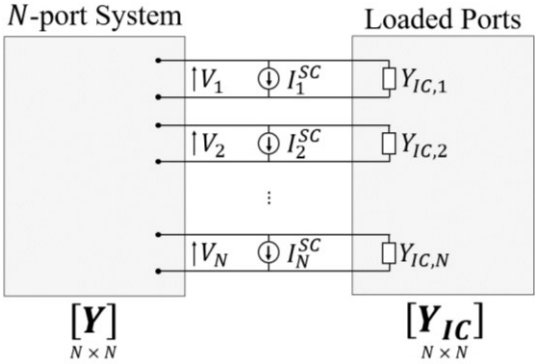

Figure 2. Norton equivalent model of a generic N-port system of an arrangement of close RFID tags, where the incident field emitted by the reader is accounted for by means of the equivalent Norton short-circuit current generators I_n^{SC} as in [21].

3 Coupled RFID Tags

To predict the sensor code values s_n in the case of coupled tags, an expression of the active input admittance Y_n^{in} of each port is required in (2). Closely coupled tags can be modeled as an N-port system [14]. However, since the *auto-tuning* equation applies to susceptances, the original formulation should be rewritten in terms of admittances by resorting to the Norton equivalent model (Fig. 2). Overall, the port's terminations are accounted for by a diagonal matrix $\boldsymbol{Y_{IC}} = \boldsymbol{G_{IC}} + j\boldsymbol{B_{IC}} = diag\left(Y_{IC,1}, \dots, Y_{IC,N}\right)$, and the general N-port system collecting the interrogating electromagnetic field is modeled by the $N \times N$ admittance matrix $\boldsymbol{Y} = \boldsymbol{G} + j\boldsymbol{B}$. By exploiting duality from [14], the most general formula of the input admittance at port n is:

$$Y_n^{in} = \sum_{k=1}^{N} Y_{nk}\frac{[\boldsymbol{Y_G^{-1}}]_k \cdot \boldsymbol{g}}{[\boldsymbol{Y_G^{-1}}]_n \cdot \boldsymbol{g}}, \tag{3}$$

where $[\boldsymbol{Y_G^{-1}}]_n$ indicates the n-th row of the inverse of the system admittance matrix $\boldsymbol{Y_G} = \boldsymbol{Y} + \boldsymbol{Y_{IC}}$ and $\boldsymbol{g}$ is the column vector of the normalized port gains[1] which groups the parameters of the system. It is worth noticing that the presence of the admittance matrix $\boldsymbol{Y_G}$ in the input admittance expression (3) produces a significant complication of the *auto-tuning* model with respect to the single-port case. In fact, the admittance matrix $\boldsymbol{Y_G}$ is affected by both the external boundary conditions ψ (e.g. the presence of several tagged items) and by the adaptive variations of each chip's admittance by means of the sensor code $s_n(\psi)$:

$$\boldsymbol{Y_G}(\psi) = \boldsymbol{Y}(\psi) + \boldsymbol{Y_{IC}}\left(\boldsymbol{s}(\psi)\right). \tag{4}$$

$\boldsymbol{s}(\psi)$ indicates the vector of the sensor codes, i.e. the status of the coupled ICs. As a consequence, the same entangled dependence falls back also for the input admittance Y_n^{in} seen at the n-th port. Hence, in the most general case, the sensor codes s_n will be the result of a non-linear system of equations.

4 Two-Port Periodic RFID Grids

For the sake of simplicity, a two-port planar RFID Grid ($N = 2$) is first considered. The following hypotheses are assumed:

(a) – The tags arrangement lays on a plane and the reader beam is in broadside with respect to the plane hosting the tags. In this case, the normalized port gain vector $\boldsymbol{g}$ becomes a vector with identical entries:

$$g_1 = g_2 = g\,.$$

(*b*) – The matrix $\boldsymbol{Y}$ is symmetric, hence the network ports have equal mutual admittances:

$$Y_{12} = Y_{21} = Y_M\,.$$

[1] For duality from [14], the normalized n-th port gain is $g_n = \sqrt{G_{nn}\, G_n(\underline{\hat{r}})\, \chi_n\, /\, \eta_0}\; e^{j\Phi_n(\underline{\hat{r}})}$, where G_{nn} is the n-th port self-conductance, G_n is the n-th port gain, and $\chi_n = \left|\underline{\hat{h}}_n \cdot \underline{\hat{h}}_R\right|^2$ and $\Phi_n = angle\left(\underline{\hat{h}}_n \cdot \underline{\hat{h}}_R\right)$ are the amplitude and the phase of the reader-port polarization mismatch, respectively.

(*c*) – The arrangement of tags shows some periodicity (even if it consists of only two elements), hence the network ports have equal self-admittances:

$$Y_{11} = Y_{22} = Y_S \,.$$

(*d*) – Provided that the system is planar, fully symmetric and broadside illuminated (as required by the previous hypotheses), the two ICs will act the same way when only two ports are present. The ICs' admittances will be therefore the same even during the automatic retuning:

$$Y_{IC,1} = Y_{IC,2} = Y_{IC} \,.$$

Accordingly, the two-port system admittance matrix $\boldsymbol{Y_G}$ reduces to:

$$\boldsymbol{Y_G} = \begin{bmatrix} Y_S + Y_{IC} & Y_M \\ Y_M & Y_S + Y_{IC} \end{bmatrix}. \tag{5}$$

This matrix becomes circulant [22], namely each row vector is rotated one element to the right w.r.t. the preceding one. For such family of matrices, the sum of the elements of each row or column is a constant: $sum[\boldsymbol{Y_G}] = const$. As a consequence, also thanks to *Hp.* (*a*), the input admittance at each port from (3) simplifies to:

$$Y_n^{in} = \sum_{k=1}^{N} Y_{nk} = Y_S + Y_M \,, \quad \forall n \,. \tag{6}$$

Note that, in the simple case of a periodic arrangement of two tags, the cross-reference between the two ICs vanishes, and the input admittance (6) becomes virtually independent on the ICs status. Therefore, the calculation of the port sensor codes (2) becomes immediate, as trivially from (6) $B_n^{in} = B_S(\psi) + B_M(\psi)\,, \forall n$, so that:

$$s_n(\psi) = S_{min} + \\ +nint\left[-\frac{1}{C_{IC,step}}\left(C_{IC}(S_{min}) + \frac{B_S + B_M}{\omega}\right)\right]. \tag{7}$$

Instead, by removing the hypothesis of periodicity (i.e. tags randomly displaced), the two input admittances are different and the sensor codes $\{s_1, s_2\}$ are the solution of the following non-linear system of 3^{rd} degree equations:

$$\begin{cases} a_1 s_1 s_2^2 + a_2 s_2^2 + a_3 s_1 s_2 + a_4 s_1 + a_5 s_2 = a_6 \\ a_7 s_1^2 s_2 + a_8 s_1^2 + a_9 s_1 s_2 + a_{10} s_1 + a_{11} s_2 = a_{12} \end{cases}, \tag{8}$$

where the multiplicative constants $\{a_1(\psi), \ldots, a_{12}(\psi)\}$ are only dependent on the changes in the boundary conditions $\psi(t)$. The system (8) admits multiple solutions, but only those for $S_{min} \leq s_n \leq S_{max}$ can be considered physically valid. In case more than a single couplet of solutions should be compatible with above conditions, following energy considerations, we conjecture that the most probable state of the ICs is the one corresponding to the smallest sensor code values, as the retuning mechanism is generated by a voltage increase at the internal varactor terminal, generated by the harvested energy.

(a) (b)

Figure 3. (a) Axzon's RFM3200-AER inlay tags [6]. (b) Two-tags Grid configuration.

5 Numerical Analysis

The above model is here applied to a set of two Axzon's RFM3200-AER tags [6] (Fig. 3.a), arranged in a symmetric configuration as in Fig. 3.b. They are dipole-like inlay tags (also enabled for temperature sensing), mounting the Magnus S3 IC [23], whose electrical parameters are: $G_{IC} = 0.482\ mS$, $C_{IC,0} = 1.9\ pF$, $C_{IC,step} = 3.1\ fF$, $S_{min} = 80$, $S_{max} = 400$. The two tags are measured in air (using a polystyrene support). The variable physical parameter ψ is the IC-to-IC distance d, which is changed between 16 mm and 121 mm, with a 5 mm pace. The interrogating linearly polarized antenna is a Voyantic log-periodic wide band antenna (AN-FF-WB) and is connected to the Jadak ThingMagic USB Pro reader. The same arrangement is also reproduced numerically by using CST Microwave Studio 2019 to evaluate the network matrix and hence estimate the sensor codes. Fig. 4.a shows the simulated input susceptance of the tags at 870 MHz. For very short inter-tag distance, the susceptance is rather disturbed w.r.t. to the

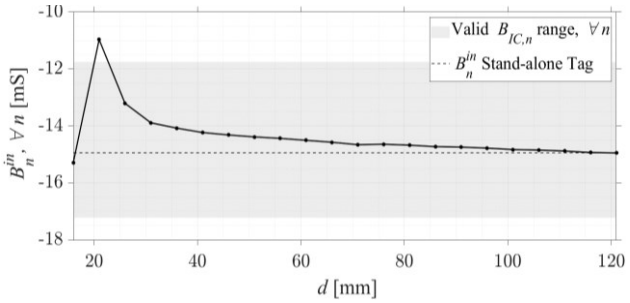

(a)

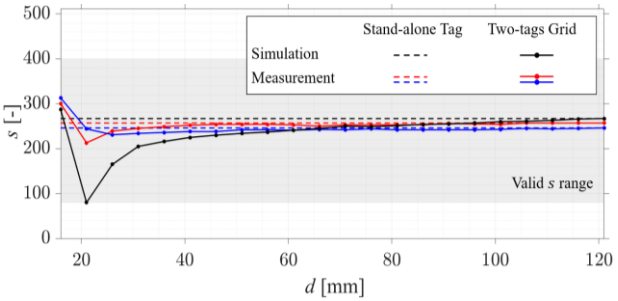

(b)

Figure 4. (a) Simulated input susceptance of the two-tags system in comparison with that of a stand-alone tag. The gray band indicates the range of the susceptance that can be retuned by the IC. (b) Simulated and measured sensor codes of the two-tags when the inter-antenna distance d is increased. Gray band indicates the useful range of the sensor code, before saturation.

standalone-tag configuration, by the effect of the electromagnetic coupling. In particular, for d close to $2\,cm$ there is a peak that goes outside the retuning capability of the chip. The corresponding simulated and measured sensor codes are presented in Fig. 4.b, also in comparison with the standalone tags. It is possible to see that both the measured sensor codes of the two tags exhibit a variation with the distance, in agreement with the numerically found profile of the susceptance. This variation reduces as the distance increases. It is worth noticing that the asymptotic values (isolated tags) are different for the two tags, due to inter-IC variability of the *auto-tuning* mechanism. The simulated behavior reproduces a similar profile as in the measurement, with correct asymptotic values. However, it tends to overestimate the effect of the mismatching, thus returning a higher variation of the sensor code for very short inter-tag distance.

6 Conclusions

A network model for electromagnetic coupled *auto-tuning* RFID tags has been presented, together with a preliminary numerical and experimental analysis. In the particular case of two tags in symmetric arrangement, the retuning effect can be predicted by closed form explicit formulas. The theoretical findings have been partly corroborated by preliminary experimentations, even if the model needs to be further refined to avoid over estimation of coupling effects.
Advances of the model, further experiments and the extensions to multiple tags will be shown at the conference.

8 References

[1] S. Monteleone, M. Sampaio and R. F. Maia, "A novel deployment of smart Cold Chain system using 2G-RFID-Sys temperature monitoring in medicine Cold Chain based on Internet of Things," *2017 IEEE International Conference on Service Operations and Logistics, and Informatics (SOLI)*, Bari, 2017, pp. 205-210

[2] Fan Jun Li and Zhao Jiong Chen, "Brief analysis of application of RFID in pharmaceutical cold-chain temperature monitoring system," *Proceedings 2011 International Conference on Transportation, Mechanical, and Electrical Engineering (TMEE)*, Changchun, 2011, pp. 2418-2420

[3] H. Ruile and P. Wunderlin, "RFID application within product life cycle of industrial textile & apparels," *RFID SysTech 2011 7th European Workshop on Smart Objects: Systems, Technologies and Applications*, Dresden, Germany, 2011, pp. 1-11

[4] Ting, J.S., Kwok, S., Tsang, A., & Lee, W., "Critical Elements and Lessons Learnt from the Implementation of an RFID-enabled Healthcare Management System in a Medical Organization", *Journal of Medical Systems 35*, 2009, pp. 657-669

[5] Y. Tanaka, Y. Umeda, O. Takyu, M. Nakayama and K. Kodama, "Change of read range for UHF passive RFID tags in close proximity," *2009 IEEE International Conference on RFID*, Orlando, FL, 2009, pp. 338-345

[6] "Axzon RFM3200 Wireless Flexible Temperature Sensor", https://axzon.com/rfm3200-wireless-flexible-temperature-sensor/

[7] "Impinj Monza R6 Tag Chip." https://www.impinj.com/products/tag-chips/impinj-monza-r6-series

[8] "Impinj M700 Series RAIN RFID Tag Chips Extend IoT", https://www.impinj.com/products/tag-chips/impinj-m700-series

[9] G. M. Bianco, S. Amendola, and G. Marrocco, "Near-Field Constrained Design for Self-Tuning UHF-RFID Antennas," *IEEE Transactions on Antennas and Propagation*, vol. 68, no. 10, pp. 6906–6911, 2020

[10] F. Amato, C. Miozzi, S. Nappi, and G. Marrocco, "Self-Tuning UHF Epidermal Antennas," *IEEE International Conference on RFID-TA*, 2019

[11] S. Amendola, C. Occhiuzzi, C. Miozzi, S. Nappi, F. Amato, F. Camera, and G. Marrocco, *UHF epidermal sensors: Technology and applications*, pp. 133–161. November 2020

[12] M. C. Caccami and G. Marrocco, "Electromagnetic Modeling of Self-Tuning RFID Sensor Antennas in Linear and Nonlinear Regimes," *IEEE Transactions on Antennas and Propagation*, vol. 66, no. 6, pp. 2779–2787, 2018

[13] G. M. Bianco and G. Marrocco, "Fingertip Self-tuning RFID Antennas for the Discrimination of Dielectric Objects," *2019 13th European Conference on Antennas and Propagation (EuCAP)*, pp. 1–4, 2019

[14] G. Marrocco, "RFID grids: Part I - Electromagnetic Theory," *Antennas and Propagation, IEEE Transactions on*, vol. 59, pp. 1019 – 1026, April 2011

[15] S. Caizzone and G. Marrocco, "RFID Grids: Part II - Experimentations," *IEEE Transactions on Antennas and Propagation*, vol. 59, no. 8, pp. 2896–2904, 2011

[16] P. V. Nikitin, S. Ramamurthy, R. Martinez and K. V. S. Rao, "Passive tag-to-tag communication," *2012 IEEE International Conference on RFID (RFID)*, Orlando, FL, 2012, pp. 177-184

[17] C. Occhiuzzi, S. Parrella, F. Camera, S. Nappi and G. Marrocco, "RFID-Based Dual-Chip Epidermal Sensing Platform for Human Skin Monitoring," in *IEEE Sensors Journal*, vol. 21, no. 4, pp. 5359-5367, 15 Feb.15, 2021

[18] Ethicheck, "COVID Vaccine Storage Solutions", https://www.ethicheck.eu/covid-solutions/

[19] G. Marrocco, "RFID-grid systems: The electromagnetic way to ubiquitous computing," 2012 *IEEE International Conference on RFID-Technologies and Applications (RFID-TA)*, Nice, 2012, pp. 303-308

[20] S. Caizzone and G. Marrocco, "RFID-grids for deformation sensing," *2012 IEEE International Conference on RFID (RFID)*, Orlando, FL, 2012, pp. 130-134

[21] G. Conciauro, *Introduzione alle onde elettromagnetiche*, 2003

[22] G. H. Golub and C. F. Van Loan, *Matrix Computations*. USA: Johns Hopkins University Press, 1996

[23] Axzon, "Magnus-S3 M3E passive sensor IC." https://axzon.com/rfm3300-e-magnus-s3-m3e-passive-sensor-ic/